

# Effect of Cross-Linking on Polymer Diffusion in Poly(butyl methacrylate-*co*-butyl acrylate) Latex Films

Toshiyuki Tamai,<sup>†</sup> Patrick Pinenq,<sup>‡</sup> and Mitchell A. Winnik\*

Department of Chemistry, University of Toronto, 80 St. George Street,  
Toronto, Ontario, Canada M5S 3H6

Received March 11, 1999; Revised Manuscript Received July 14, 1999

**ABSTRACT:** The effect of cross-linking on intercellular polymer diffusion in poly(butyl methacrylate-*co*-butyl acrylate-*co*-ethylene glycol dimethacrylate) latex films containing 0.1–4 mol % ethylene glycol dimethacrylate (EGDMA) as a cross-linking agent was monitored by fluorescent energy-transfer measurements and by atomic force microscopy. The presence of cross-links in the latex particles limits the extent of polymer interdiffusion. The extent of mixing caused by this polymer diffusion decreased with increasing levels of cross-linking. Even, however, in films containing 4 mol % EGDMA, significant polymer diffusion occurred. To explain polymer diffusion in latex films with 100% gel content, we imagine that the intercellular mixing is caused by diffusion of dangling polymer chains anchored in the cross-linked network. These cross-linked latex particles form tough elastomeric films (with  $T_g$  estimated to be 10 °C), characterized by high tensile strength and substantial elongation to break (>100% elongation). The films have poor resistance to organic solvents.

## Introduction

When a dispersion of soft latex particles in water is allowed to dry, the particles become deformed into space-filling (Voronoi) polyhedra, which pack together to form a void-free and transparent film.<sup>1,2</sup> The newly formed film has poor mechanical properties because of weak adhesion at the interface between adjacent cells. Strength is acquired over time or with annealing as a consequence of polymer diffusion across the boundary between adjacent cells. In this way, mechanically coherent films are formed. Polymer diffusion across an interface to generate mechanical strength through the formation of entanglements is a feature common to polymer welding, crack healing, and the compression molding of polymer powders. The process of polymer diffusion to generate entanglements is said to “heal” the interface.

While latex coatings normally display excellent performance in many application areas, they generally have poorer chemical and solvent resistance and lower tensile strength and hardness than traditional solvent-borne coatings which cross-link on the substrate. Introducing cross-links into a latex film can increase its physical and chemical stability, as well as improve its tensile strength and abrasion resistance.<sup>3</sup> As a consequence, there is a deep and growing interest within the coatings industry in cross-linked water-borne coatings.

There are two ways in which one can introduce cross-links into a latex coating. One can introduce chemical functionality into the latex particle, along with catalysts or coreactants in the dispersion, so that cross-linking occurs after the coating is applied to the substrate. Traditional *N*-methylolacrylamide coatings and latex coatings based upon melamine derivatives operate in

this way. Alternatively, one can introduce cross-links into the latex particle itself.<sup>4–7</sup> There is, however, evidence in the scientific literature to suggest that this is not a wise strategy. Zosel and Ley<sup>5</sup> have shown that introduction of 2% of methallyl methacrylate (MAMA) into the feed in the emulsion polymerization of butyl methacrylate (BMA) has a profound effect on films formed from the latex. Newly formed films of both PBMA and P(BMA-*co*-MAMA) are brittle, but upon annealing at 90 °C, the PBMA films develop substantial toughness as exhibited by tensile measurements. Films formed from the cross-linked copolymer latex remain brittle even after substantial annealing at 90 °C. Hahn, Ley, and Oberthur<sup>6</sup> used small-angle neutron scattering (SANS) experiments to show that the diffusion of uncross-linked deuterated PBMA is retarded significantly in latex blend films in which the PBMA-*d* is mixed with an excess of cross-linked P(BMA-*co*-MAMA). We know from the classic experiments of Ahagon and Gent<sup>8</sup> that when two cross-linked polymers are brought together at a temperature above their glass transition temperature  $T_g$ , polymer diffusion across the interface to generate adhesion through formation of entanglements is restricted to chain segments dangling from the network.

It is, however, relatively common practice in industry to employ cross-linked latex particles in coatings formulations. In this paper, we return to this subject, carrying our experiments analogous to those reported by Ley and co-workers,<sup>5,6</sup> but with a latex polymer that is an elastomer at room temperature. We examine butyl methacrylate–butyl acrylate copolymer films, for which the  $T_g$  is estimated to be 10 °C. We introduce donor and acceptor groups into the latex to allow us to study the extent of polymer diffusion by energy-transfer measurements and introduce different levels of cross-linking by use of varying amounts of ethylene glycol dimethacrylate (EGDMA). We find that annealed films prepared from particles containing even 4 mol % EGDMA exhibit substantial toughness and elongation to break when tested at room temperature. Not surprisingly, these

<sup>†</sup> Permanent address: Osaka Municipal Technical Research Institute, 1-6-50 Morinomiya, Joto-ku, Osaka 536-8553, Japan.

<sup>‡</sup> Permanent address: Elf-Atochem, Centre d'Applications de Lavallois, 95, rue Danton, F-92300 Lavallois-Perret, France.

\* To whom correspondence should be addressed: e-mail mwinnik@chem.utoronto.ca.

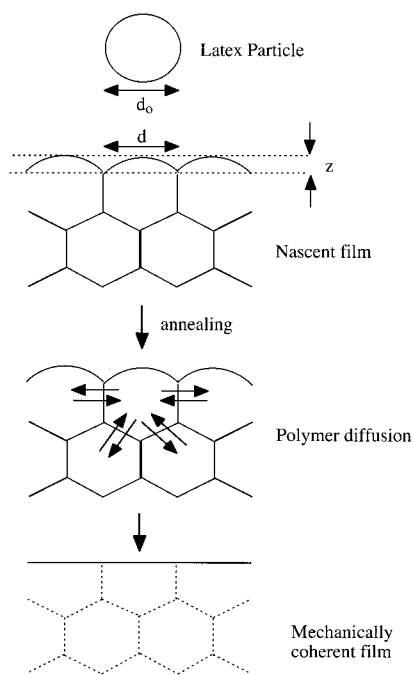


**Figure 1.** A representation of the film formation process, showing a cross section of the latex film at the surface.  $d_0$  is the diameter of a latex particle dispersed in water,  $d$  is the width of a cell inside the latex film, and  $z$  is the peak-to-valley height difference. The arrows refer to diffusion of polymer molecules across the cell boundaries.

films show poor solvent resistance. We examine the evolution of film surface topography by atomic force microscopy<sup>7,9,10</sup> and find large effects related to the extent of cross-linking in the latex from which the films are formed.

A drawing describing these processes for a latex film is presented in Figure 1. In the nascent film, particles trapped within the interior of the film are compressed into space-filling polyhedra, represented by the hexagons in the drawing. At the particle surface, only limited deformation occurs. Techniques such as atomic force microscopy allow one to observe the spherical cap structures, vestiges of the original latex particles. Inter-cellular polymer diffusion can occur once the adjacent cells come into intimate contact. In this paper, we consider how the presence of different levels of cross-linking in the latex particles affects their deformation during film formation, the extent of polymer diffusion between adjacent cells, and the development of tensile strength in the films.

## Experimental Section

**Materials.** 9-Anthryl methacrylate (AnMA) and 9-vinylphenanthrene (V-Phe) were synthesized as described previously.<sup>11,12</sup> Butyl methacrylate (BMA), butyl acrylate (BA), and ethylene glycol dimethacrylate (EGDMA) (all Aldrich) were distilled under vacuum prior to use. Potassium persulfate (KPS, Aldrich) and sodium dodecyl sulfate (SDS, Acros) were used as received. Distilled water was further purified through a Millipore Milli-Q system.

**Latex Preparation.** All latex dispersions were prepared by seeded semicontinuous emulsion polymerization under monomer-starved conditions.<sup>13</sup> An unlabeled seed was prepared by batch emulsion polymerization and used for the preparation of a series of phenanthrene (Phe)- or anthracene (An)-labeled latex samples. The seed commonly represents about 10 wt % of the final latex. A typical example is given below, and typical recipes are given in Table 1.

**Table 1. Recipes for the Preparation of Cross-Linked Latex Dispersions**

	first stage	second stage
BMA	31.95 g	15.98 g
BA	3.2 g	1.6 g
EGDMA	0.99 g	0.025 g <sup>a</sup>
V-Phe (AnMA)		0.255 g (0.328 g)
seed dispersion		30 g
SDS	2.52 g	0.3 g
KPS	0.76 g	0.03 g
water	730 mL	13.5 mL
temp	80 °C	80 °C
time	2 h	14 h <sup>b</sup>

<sup>a</sup> 0.1 mol % based on total monomer. For other reactions, 0.123 g (0.5 mol %), 0.248 g (1 mol %), 0.493 g (2 mol %), 0.986 g (4 mol %). <sup>b</sup> Second stage reactants were fed into reaction flask over 12 h. The reaction was then stirred for another 2 h at 80 °C.

**Table 2. Recipes for the Preparation of Non-Cross-Linked Latex Dispersions**

	first stage	second stage	third stage
BMA	5.45 g	14.58 g	13.68 g
BA	0.53 g	1.43 g	1.34 g
V-Phe (AnMA)			0.119 g (0.14 g)
seed dispersion		43.8 g <sup>a</sup>	8.25 g <sup>b</sup>
SDS	0.9 g	0.076 g	0.3 g
KPS	0.18 g	0.06 g	0.03 g
water	150 mL	40 mL	30 mL
NaHCO <sub>3</sub>	0.18 g		
temp	80 °C	80 °C	80 °C
time <sup>c</sup>	2 h	14 h	14 h

<sup>a</sup> Dispersion obtained by the batch emulsion polymerization.

<sup>b</sup> Dispersion obtained in the second stage polymerization. <sup>c</sup> Second and third stage reactants were fed into the reaction flask over 12 h. The reaction was then stirred for another 2 h at 80 °C.

A 1 L flask equipped with a condenser and mechanical stirrer was filled with water (730 mL), BMA (31.95 g), BA (3.2 g), EGDMA (0.99 g), sodium dodecyl sulfate (SDS, 2.52 g), and sodium potassium persulfate (KPS, 0.76 g). The solution was purged with nitrogen gas for 2 h and then heated to 80 °C for an additional 2 h. This produced a solution (4.7 wt % by gravimetric analysis) of particles with a diameter (dynamic light scattering) of 47 nm and a narrow size distribution. In the second-stage polymerization, a portion of the seed dispersion (30 g) was introduced into the reaction flask and purged with nitrogen for 15 min. The flask was heated to 80 °C under N<sub>2</sub>, and two solutions were then fed into the flask at a constant rate over 12 h. One contained the monomers BMA (15.98 g), BA (1.6 g), EGDMA (0.1–4 mol % of the total monomer), and a fluorescent comonomer (AnMA or V-Phe, 1 mol % of the total monomer). The second solution contained surfactant SDS (0.3 g) and initiator KPS (0.03 g) in water (13.5 mL). Stirring at 80 °C was continued for 12 h during the feed of reactants, plus an additional 2 h, before cooling the flask and its contents to room temperature. This reaction produced dispersions at 28–32 wt % solids content and particle diameters of 93–116 nm, each with a narrow size distribution. Particle sizes and the size distributions were measured by dynamic light scattering employing a Brookhaven BI-90 particle sizer.

The particle sizes obtained were as follows: latex containing 0.1 mol % EGDMA: 95 nm (Phe-labeled), 97 nm (An-labeled); 0.5 mol % EGDMA: 98 nm (Phe-labeled), 95 nm (An-labeled); 1 mol % EGDMA: 120 nm (Phe-labeled), 114 nm (An-labeled); 2 mol % EGDMA: 93 nm (Phe-labeled), 102 nm (An-labeled); 4 mol % EGDMA: 116 nm (Phe-labeled), 110 nm (An-labeled). The un-cross-linked latex particles (without EGDMA), synthesized in conjunction with a different project,<sup>14</sup> were also prepared by seeded semicontinuous emulsion polymerization (cf. Table 2). The particle diameters and molecular weights are as follows: Phe-labeled particle, 151 nm,  $M_w = 2.8 \times 10^5$ ,  $M_w/M_n = 3.3$ ; An-labeled particle, 150 nm,  $M_w = 2.8 \times 10^5$ ,  $M_w/M_n = 3.3$ . Molecular weights were determined for filtered solutions of the polymer in tetrahydrofuran by gel permeation

chromatography (GPC) relative to poly(methyl methacrylate) standards. These samples have a measurable gel content (32%, see below); the molecular weights refer to the soluble fraction of the polymer.

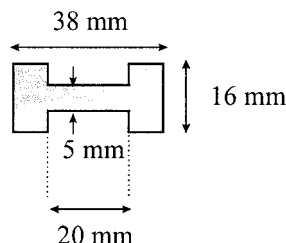
**Film Formation and Characterization.** Each dispersion was cleaned by ion exchange to remove surfactant and other water-soluble ionic materials prior to film formation. The ion-exchange resin (Bio-Rad AG 501-X8) was washed with hot deionized water ( $>80^{\circ}\text{C}$ ), methanol, and deionized water before use. Twice the weight of the resin, based upon the weight of solid present in the dispersion to be cleaned, was added to the diluted latex dispersion (solids content about 5 wt %), and then the mixture was stirred at room temperature for about 24 h. Over this time, the viscosity of the dispersion increased and the dispersion became opalescent, indicating formation of colloidal crystalline domains. The ion-exchange resin was removed by gravity filtration. All films prepared in these experiments except the tensile test employed latex dispersions cleaned by ion exchange. As shown elsewhere,<sup>14</sup> purifying this type of latex dispersion in this way has no measurable effect on the rate of polymer diffusion.

The extent of cross-linking was characterized by solvent extraction. Film specimens (weight  $W_0$ , dimensions  $20 \times 20 \times 0.1$  mm) were immersed in 1,4-dioxane for 48 h at room temperature. Each solution was filtered through a filter paper to collect the gel portion of the swollen film. The films and collected gel were then dried to a constant weight ( $W_1$ ) under vacuum in a vacuum oven. The gel content (percent) is calculated from  $W_1/W_0 \times 100$ . The solvent-swollen films were too fragile to carry out a meaningful determination of the swell ratio.

For polymer diffusion analysis by direct nonradiative energy transfer, a few drops of a dispersion containing equal amounts of Phe-labeled and An-labeled latex were put on a small quartz plate ( $20 \times 10$  mm) and then placed in an air-flushed oven prewarmed to  $30^{\circ}$  for 8–10 h. The quartz plate was covered with Petri dish in order to slow the drying process. Transparent films 40–90  $\mu\text{m}$  thick were formed over a period of ca. 6 h. Films on their substrates to be annealed were placed directly on a high mass aluminum plate in an oven preheated to the annealing temperature. For fluorescence decay measurements, the labeled films were placed in a quartz tube and degassed with  $\text{N}_2$ .

The atomic force microscope (AFM) used is a commercial instrument (Nanoscope III, Digital Instruments) operated in the contact mode. Films of ca. 20  $\mu\text{m}$  thickness were prepared by putting a few drops of the latex dispersion onto ca. 10 mm square plate of freshly cleaved mica. The films were dried at  $30^{\circ}\text{C}$ . After the newly formed films were examined by AFM, they were annealed at  $80^{\circ}\text{C}$  in an oven.

The mechanical strength of some of the films was characterized by stress-strain measurements with a Sintech 1 (MTS Systems Corp.) tensile tester.<sup>13</sup> Individual films with thicknesses in the range 0.6–0.9 mm were obtained by drying a latex dispersion very slowly at high humidity over 3 days at  $40^{\circ}\text{C}$ . Standard tensile test specimens were cut from the latex films using a metallic die (similar to that described in ASTM D1707-84). The tensile tests were carried out in a room in which the temperature and humidity were kept constant and monitored ( $21^{\circ}\text{C}/50\%$  humidity). Some films were annealed at  $80^{\circ}\text{C}$  prior to transfer to the humidity-controlled room. The cut specimens had the following shape:



The test specimen were placed in the test room 24 h prior to carrying out the tensile measurements in order to allow the

samples to equilibrate with the room temperature and humidity. The testing machine was equipped with pneumatic clamps. In this way the pressure applied on the specimen remained constant throughout the test and constant from sample to sample.

The deformation was followed by recording the cross-head displacement, employing a displacement speed of 19 mm/min. For each type of film, tensile tests were repeated on four samples to assess the reproducibility and to calculate the standard deviations for the measurement. From the stress-strain curves, the stress-at-break  $\sigma_b$  and the strain-at-break  $\lambda_b$  were determined, and the toughness  $W$  was obtained by calculating the area under the each stress-strain curve.

**Fluorescence Decay Measurements.** Fluorescence decay measurements were carried out as described previously,<sup>11–15</sup> and the areas under each decay curve were integrated and analyzed as described below. The characteristic (Förster) energy transfer distance for phenanthrene (Phe, donor) and anthracene (An, acceptor) is 23 Å.<sup>15</sup> The phenanthrene group was excited at 298 nm, and its emission was recorded at 350–360 nm.

A useful measure of the extent of energy transfer (ET) in the system is the quantum efficiency of energy transfer  $\Phi_{\text{ET}}$ , which we calculate from the donor fluorescence decay profiles  $I_D(t)$  for films in the presence and absence of acceptor.

$$\Phi_{\text{ET}} = 1 - \frac{\int_0^\infty I_D(t) dt}{\int_0^\infty I_D^0(t) dt} = 1 - \text{Area}(t)/\text{Area}_D^0 \quad (1)$$

The middle term represents the definition of the energy-transfer efficiency in terms of the integrated intensity decay profiles, where the  $I_D^0(t)$  is the donor decay profile in the absence of acceptor. For latex films containing only phenanthrene and no acceptor,  $I_D^0(t)$  is always exponential.  $\text{Area}(t)$  represents the integrated area under the fluorescence decay profile of a latex film sample annealed for a time  $t$ , and  $\text{Area}_D^0$  refers to the area under the decay profile of a film containing no acceptor. To calculate  $\text{Area}(t)$  values, the nonexponential decay profiles are fitted to the stretched exponential in eq 2.

$$I_D(t) = B_1 \exp[-t/\tau^0 - P(t/\tau^0)^{1/2}] + B_2 \exp(-t/\tau^0) \quad (2)$$

The fitting parameters  $B_1$ ,  $B_2$ , and  $P$  in eq 2 obtained from each profile are useful for area integration, but their physical meaning is not important here. These integrated areas have dimensions of time and define an average decay time  $\langle\tau_D\rangle$  for the sample. The area under the  $I_D^0(t)$  decay profile is the unquenched fluorescence decay time  $\tau^0$ .

## Results and Discussion

**Latex Synthesis and Film Formation.** The copolymer P[BMA-co-BA] (9:1) was chosen as the base polymer, because it has a glass transition temperature ( $T_g$ ) below room temperature and is able to form transparent films under ambient conditions. The  $T_g$  of the polymer without cross-linking agent is estimated to be  $10^{\circ}\text{C}$  from the Fox equation.<sup>16</sup> Low levels of cross-linking have only a small effect on the  $T_g$  of the polymer. A series of latex dispersions containing 0.1–4 mol % EGDMA as a cross-linking agent were synthesized. Particle diameters ranged from 93 to 102 nm. All latex particles were labeled with 1 mol % phenanthrene or anthracene groups for direct nonradiative energy-transfer (ET) studies.

The films were cast on quartz plates, dried slowly at  $30^{\circ}\text{C}$ , and annealed at  $80^{\circ}\text{C}$  to promote healing of the interfaces. All of the films prepared were transparent and free of cracks. The gel content of each of the latex films was measured in order to determine the extent of cross-linking (cf. Table 3). Films without EGDMA also

**Table 3. Fraction of Mixing ( $f_m$ ), Quantum Efficiency of Energy Transfer ( $\Phi_{ET}$ ), and Gel Content of Latex Films**

EGDMA (mol %)	$f_m$ (max) <sup>a</sup>	$\Phi_{ET}(0)$ <sup>b</sup>	$\Phi_{ET}(\text{max})$ <sup>c</sup>	gel content (%)
0 <sup>d</sup>	1	0.009	0.41	32
0.1	0.83	0.19	0.55	41
0.5	0.43	0.20	0.37	100
1	0.32	0.16	0.31	89
2	0.10	0.11	0.16	90
4	0.09	0.13	0.17	87

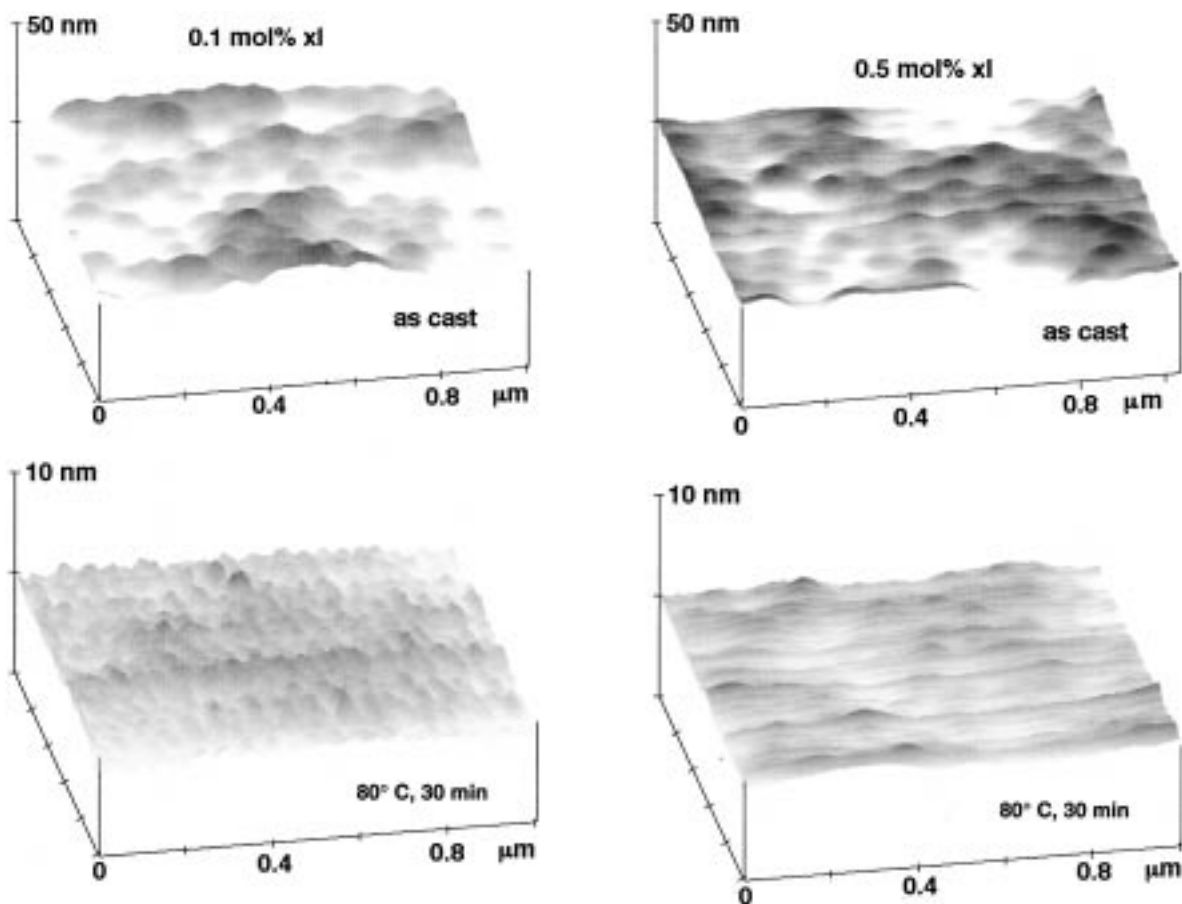
<sup>a</sup> The maximum value of the fraction of mixing for the annealed films. <sup>b</sup> Quantum efficiency of energy transfer for the nascent films. <sup>c</sup> The maximum value of efficiency of energy transfer for the annealed films. <sup>d</sup> Film prepared from a latex dispersions that has a larger particle diameter (151 nm) and a lower content (0.5 mol %) of donor and acceptor dyes than the other dispersions.

gave some gel (32 wt %). Cross-linking can occur naturally with BA as a comonomer.<sup>5,17</sup> When we tried to measure swell ratios, however, the films swollen with solvent were very fragile. They broke up into tiny fragments that made it difficult to obtain reproducible values of the swell ratio. The films containing 0.5–4 mol % EGDMA had high gel contents. Given the fragile nature of the films and the possibility that small amounts of gel fragment might pass through the filter paper used to collect the solvent-swollen gel, the values in Table 3 for these latex are indistinguishable from 100% gel content.

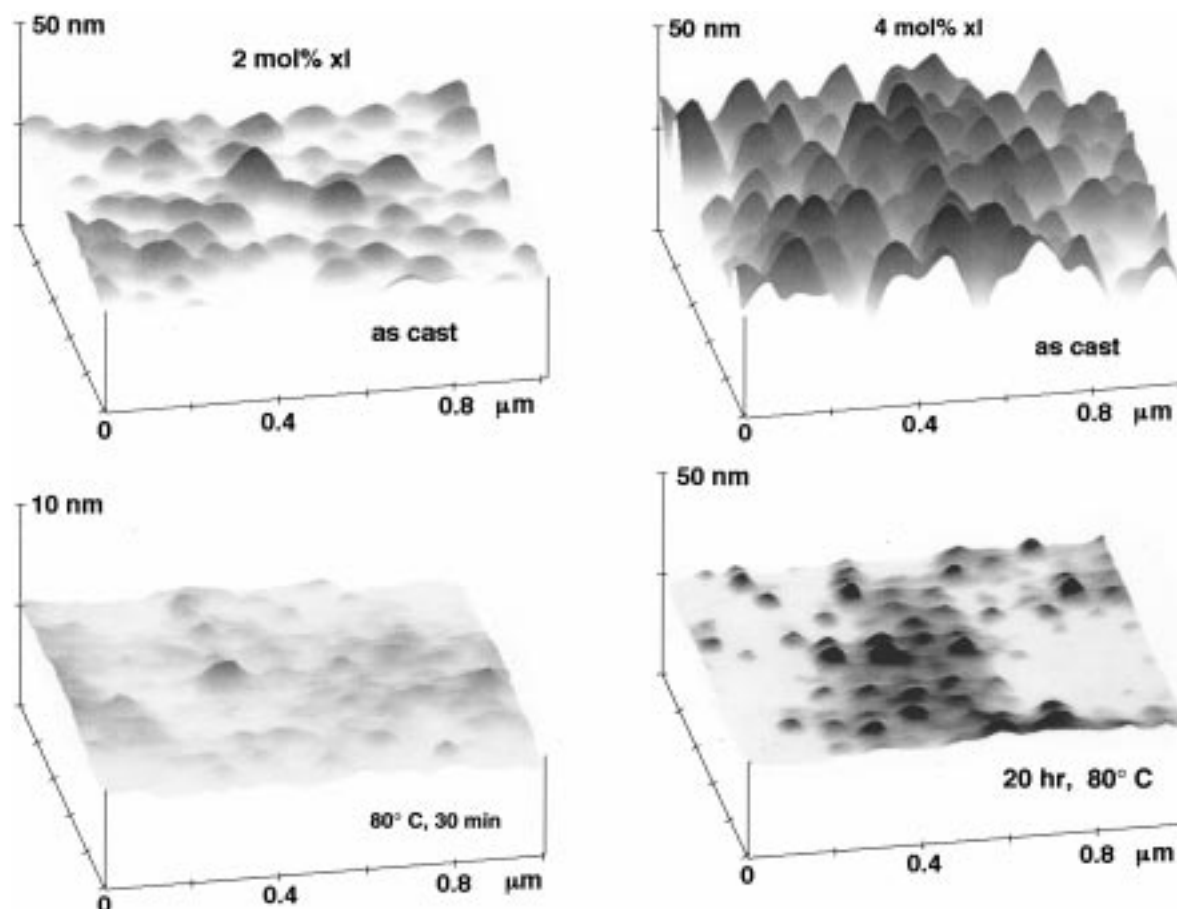
**Surface Morphology.** The morphology of the film surfaces was examined by atomic force microscopy (AFM). Both nascent films and annealed films were examined to try to detect the effect of annealing. An

image of a nascent latex film containing 0.1 mol % EGDMA is shown in the upper left-hand part of Figure 2. The peak-to-valley distance ( $z$ ) is in the range 3–5 nm, which is much smaller than half of a latex particle diameter. The surface features of the film formed from the 0.5 mol % EGDMA latex look very similar (Figure 2, upper right). During film formation, these latex particles were deformed by the capillary and surface tension forces that accompany the drying process,<sup>18,19</sup> to give Voronoi polyhedra in the bulk and undulations at the surface, as shown in Figure 1. In all of the films we examined, the surfaces exhibited an ordered array of cells with the same characteristic width ( $d = 100$  nm) as that of the diameter ( $d_0$ ) of the particles from which they were formed. When both films are annealed for 30 min at 80 °C, much of the surface roughness disappears. The films are essentially flat, with mild undulations on the scale of  $\pm 1$ –2 nm, and all vestiges of the original cellular structure are lost.

Increasing the amount of EGDMA leads to a more pronounced surface roughness (Figure 3). The peak-to-valley distance increases with the increase in EGDMA content: 12 to 18 nm (2 mol %), 30 to 40 nm (4 mol %). These surfaces were also imaged by AFM after annealing the films. In the latex films containing 2 mol % EGDMA, the deformation was complete after 0.5 h at 80 °C. In contrast, the deformation of latex particles containing 4 mol % EGDMA took place less efficiently. Undulations were observed by AFM even after 20 h annealing, although the peak-to-valley distance decreased to about 2–3 nm.



**Figure 2.** Surface images of latex films prepared from particles containing 0.1 and 0.5 mol % EGDMA (xl) observed by atomic force microscopy: top, nascent films; bottom, films annealed at 80 °C for 0.5 h.



**Figure 3.** Surface images of latex films containing 2 and 4 mol % EGDMA observed by atomic force microscopy: top, nascent film; bottom, films annealed at 80 °C for 0.5 h (2 mol % EGDMA) and 20 h (4 mol % EGDMA).

Similar surface undulations of non-cross-linked PBMA and other latex films were observed previously by AFM.<sup>9,10</sup> To explain the relatively rapid evolution of the film surface accompanying annealing of PBMA latex films, Goh et al.<sup>10</sup> concluded that polymer diffusion at the film surface is much faster than that inside the bulk of the film.

**Polymer Diffusion.** We monitored the polymer diffusion process by measuring changes in the extent of direct nonradiative energy transfer (ET) from a donor dye (phenanthrene: Phe) to an acceptor dye (anthracene: An) attached to the latex polymers. Fluorescence decay measurement were carried out on films as a means of assessing the extent of ET as a function of annealing history. In newly formed films, Phe and An are separated in individual cells. Polymer diffusion during annealing mixes the Phe- and An-labeled polymers between adjacent cells, bringing the two chromophores into proximity. Latex films containing only Phe as fluorescent label exhibited an exponential fluorescence decay; the lifetimes ( $\tau^0$ ) were 44.7 ns (0.1 mol %), 44.2 ns (0.5 mol %), 45.5 ns (1 mol %), 44.6 ns (2 mol %), and 44.8 ns (4 mol %). Latex films prepared from a 1:1 mixture of Phe- and An-labeled latex dispersions exhibited nonexponential fluorescence decay profiles because of ET from Phe to An in the film. Even in freshly prepared films, the fluorescence decay profiles  $I_b(t)$  exhibited deviations from a strictly exponential decay profile. Nonexponential decays in these films are due primarily to ET across the interparticle boundary, although for low- $T_g$  latex, some polymer diffusion can occur during film formation.<sup>20</sup> Here films are formed at

30 °C, about 20 °C above the estimated  $T_g$  of latex polymer. Under these circumstances, the extent of polymer diffusion occurring during film formation is small.

The quantum efficiency of energy transfer  $\Phi_{ET}$  for each sample was calculated from eq 1. Values of  $\Phi_{ET}$  allow one to monitor the extent of ET in latex film without assuming a specific model to parametrize the  $I_b(t)$  decay profile. The values of  $\Phi_{ET}(0)$ , which we attribute to trans-boundary ET upon nascent films, will depend on the contact area between donor- and acceptor-labeled particles and the concentration of label. We have shown previously that, in immiscible polymer blend films consisting of donor- and acceptor-labeled components,  $\Phi_{ET}(0)$  increases with the increase of the interfacial contact area between two components.<sup>21</sup>

To calculate the "extent of mixing"  $f_m$  that occurs upon annealing the samples, we have to correct for trans-boundary ET and other contributions to ET in the newly formed films. We define  $f_m$  as

$$f_m = f_m(t) = \frac{\Phi_{ET}(t) - \Phi_{ET}(0)}{\Phi_{ET}(\infty) - \Phi_{ET}(0)} = \frac{\text{Area}(0) - \text{Area}(t)}{\text{Area}(0) - \text{Area}(\infty)} \quad (3)$$

where  $[\Phi_{ET}(t) - \Phi_{ET}(0)]$  represents the change in ET efficiency between the initially prepared film and that aged for time  $t$ .<sup>22</sup> Strictly speaking,  $f_m$  represents the "quantum fraction" of mixing rather than the mass fraction of mixing  $f_s$ . This distinction would be important if we were to attempt to calculate from the data the depth of penetration of the polymers or polymer seg-

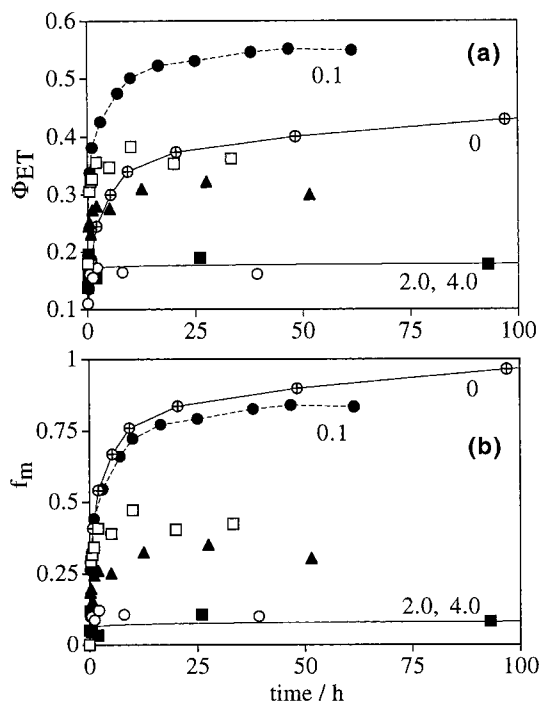


**Figure 4.** Plots of (a)  $\Phi_{ET}$  (quantum efficiency of energy transfer) vs annealing time and (b)  $f_m$  (fraction of mixing) vs annealing time, for latex films containing 0 (○), 0.1 (●), 0.5 (□), 1 (▲), 2 (○), and 4 mol % (■) EGDMA.

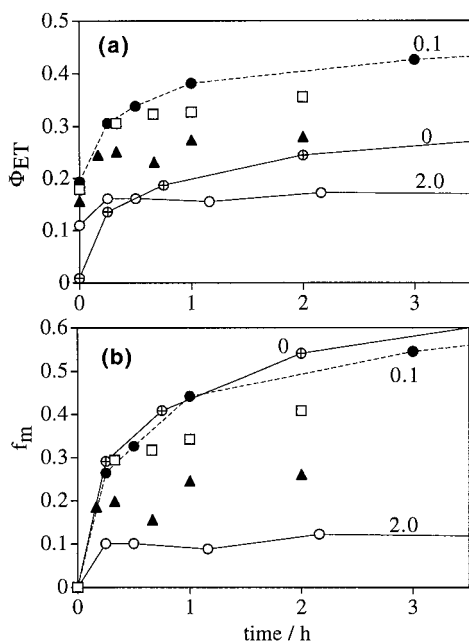


**Figure 5.** Plots of (a)  $\Phi_{ET}$  (quantum efficiency of energy transfer) vs annealing time and (b)  $f_m$  (fraction of mixing) vs time, for relatively short annealing times, for latex films containing 0 (○), 0.1 (●), 0.5 (□), 1 (▲), and 2 mol % (○) EGDMA.

ments that diffuse across the interparticle boundary. We note that in simpler systems  $f_s$  is proportional to  $f_m$  for  $f_m$  values up to ca. 0.7.<sup>23</sup>

Freshly formed latex films were annealed at 80 °C. We plot the values of  $\Phi_{ET}$  and  $f_m$  vs annealing time for latex films containing 0.1–4 mol % EGDMA in Figures 4 and 5. The values of  $\Phi_{ET}$  and  $f_m$  increase with time and level off at long annealing times.

We also plot the results for a non-cross-linked latex film (without EGDMA) for comparison. The non-cross-

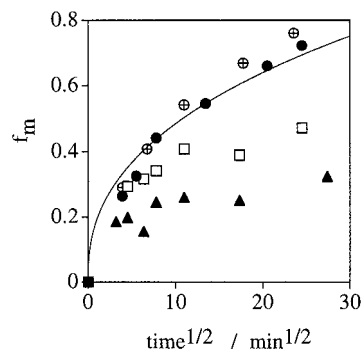


**Figure 6.** Plots of  $f_m$  (fraction of mixing) vs  $(\text{time})^{1/2}$  during the early stages of annealing for latex films containing 0 (○), 0.1 (●), 0.5 (□), and 1 mol % (▲) EGDMA.

linked latex particles have a larger particle diameter (151 nm) and a lower concentration (0.5 mol %) of donor and acceptor dyes than those of cross-linked particles (ca. 100 nm, 1 mol %).<sup>12</sup> The lower concentration of dyes and smaller contact area between each particles leads to a lower efficiency of ET, especially in the nascent film with only trans-boundary ET (Table 3). The  $\Phi_{ET}$  values for non-cross-linked nascent latex film were lower than those for films formed from the other latex dispersions, and the values obtained after annealing were also much lower than those containing 0.1 mol % EGDMA. This result emphasizes that one cannot compare directly  $\Phi_{ET}$  values in systems containing different levels of labeling. In contrast, the  $f_m$  values were comparable for both systems. The  $f_m$  values of the non-cross-linked latex film increased faster with annealing time and continued to increase for longer times than that for the film of cross-linked latex polymer. For the cross-linked latex films,  $f_m$  values approach a limiting value less than unity, whereas for the non-cross-linked films,  $f_m$  always reaches unity (full mixing). In the so-called “un-cross-linked” film examined here, the relatively small gel content (32%) did not interfere with the approach of  $f_m$  to its limiting value of unity. Full mixing, as determined by these ET experiments, corresponds to polymer diffusion over distances comparable to a particle radius. Taken together, these results indicate to us that  $f_m$  is an appropriate parameter to monitor the extent of polymer mixing in these systems.

Figures 4 and 5 indicate that increasing amounts of EGDMA slow the growth in time of  $\Phi_{ET}$  and  $f_m$  and also limit their maximum values. More surprising is the important result that a significant extent of mixing of polymer occurs even in the latex films that contains 2 and 4 mol % EGDMA.

In many previous examples of latex films examined in our laboratory, we have found that the growth of  $f_m$  was proportional to  $t^{1/2}$  for a significant fraction of the total mixing in cases where the weight-averaged molecular weight of the latex polymer was not much higher than the estimated entanglement molecular weight.<sup>24</sup> In Figure 6 we present plots of  $f_m$  vs  $t^{1/2}$  for the latex films described above. In none of these samples does  $f_m$  increase linearly with  $t^{1/2}$ . Even for the non-cross-linked latex ( $M_w = 2.8 \times 10^5$ ) the growth in  $f_m$  is not proportional to  $t^{1/2}$ . For this sample we have two complicating features of the system:  $M_w$  (as determined by GPC) is high, and there is a measurable gel content in the system.

**Tensile Measurements.** Tensile strength measurements were carried out on latex films prepared from

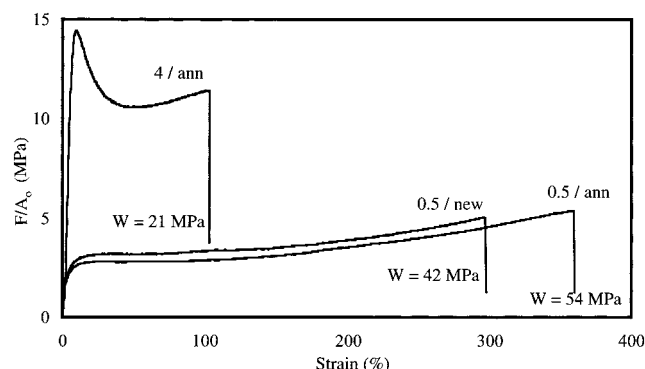


**Figure 7.** Representative stress-strain ( $F/A_0$  vs  $\lambda$ ) curves for thick latex films (ca. 0.6 mm) dried at 40 °C over 3 days. The sample 0.5/new refers to the film containing 0.5 mol % EGDMA transferred to a humidity-controlled room after removal from the drying oven. The sample 0.5/ann refers to a similar film annealed for 48 h at 80 °C prior to transfer to the humidity-controlled room after removal from the drying oven. The sample 4/ann refers to a film containing 4 mol % EGDMA annealed for 90 h at 80 °C. The toughness  $W$  is calculated as the area under the each stress-strain curve, taking account of the decrease in cross section as the film is elongated.

particles containing 0.5 and 4 mol % EGDMA as a cross-linking agent. A more detailed examination of films prepared from the un-cross-linked latex and the latex containing 1 mol % EGDMA is described in ref 14. To obtain defect-free films with a smooth surface, the dispersions were dried very slowly at high humidity, over 3 days at 40 °C. The films were subsequently aged for 24 h at 21 °C at 50% relative humidity. Under these conditions, a significant extent of polymer diffusion occurs. Films formed from the un-cross-linked latex and from the latex prepared with 0.5 mol % EGDMA and 1 mol % EGDMA (see ref 14) exhibit high elongation to break (>300%) and substantial toughness. Estimated standard deviations in these values are on the order of  $\pm 10\%$ .<sup>14</sup> In Figure 7, we compare results (representative traces) for the films containing 0.5 and 4 mol % EGDMA. To emphasize features occurring at small deformation, we prefer to plot stress values calculated as the measured force divided by the initial cross-sectional area ( $F/A_0$ , the so-called "engineering stress"). At high strain, the films become thinner; the cross-sectional area decreases. This change has to be taken into account when calculating the toughness of the film as the integrated area under the stress-strain curve.

In Figure 7 we see that the unannealed film with 0.5 mol % cross-linker has a strain-at-break  $\lambda_b$  of ca. 300%. When the film with 0.5 mol % cross-linker is annealed for 48 h at 80 °C, both the strain at break and the toughness increase significantly. The values for  $\lambda_b$  and the toughness for this film are slightly smaller than corresponding values of the un-cross-linked film. The corresponding unannealed film with 4 mol % cross-linker is too fragile to measure. When heated for 90 h at 80 °C, these films exhibit a substantial yield stress and tensile strength. Even for this relatively highly cross-linked latex, the films are elastomeric and stretch to twice their initial length before breaking.

**Effect of Cross-Linking on Film Formation and Annealing.** In the classical mechanism of film formation from latex dispersions, the latex particles dispersed in water are deformed by capillary forces during water evaporation. As adjacent particles approach and touch, forces associated with surface tension bring adjacent cells into intimate contact, with locally flat surfaces

separating the Voronoi polyhedra inside the film.<sup>25</sup> When the latex particles consist of only linear polymer, deformation strains accompanying film formation will relax with a rate determined by the terminal relaxation time of the polymer. For cross-linked particles, the deformation is elastic and imparts a decrease in entropy that cannot fully relax, even through the diffusion of polymer segments and dangling ends.<sup>18,19</sup>

In our system, increasing the amount of cross-linking agent in the latex affects the extent of particle deformation at the surface of newly formed films. AFM measurements show that the surface of films containing 2 and 4 mol % EGDMA are relatively rough. The relatively large peak-to-valley ratios for these films indicate that the presence of cross-links increases the resistance of particles to deformation. Energy-transfer experiments also show that the quantum efficiencies of energy transfer  $\Phi_{ET}(0)$  of films containing 2 and 4 mol % EGDMA are smaller (Table 3) than those of films formed of less tightly cross-linked latex. If the deformation of latex particles inside the film is incomplete, so that small voids (interstitial space between particles) exist, the contact area between each particle becomes smaller. Even voids that are much too small (1–2 nm) to scatter light will decrease the efficiency of trans-boundary energy transfer.<sup>21</sup> Both sets of results suggest that cross-linking limits the deformation of the latex during the film formation, both at surface and in the interior of the film. The effect at the surface of the film is much more pronounced.

Intercellular polymer diffusion can begin only once adjacent cells come into contact.<sup>26</sup> There is evidence to suggest that this contact does not occur until the films are nearly completely dry.<sup>20</sup> Even for polymers for which  $T_g$  is lower than the film formation temperature, the extent of polymer diffusion prior to drying is relatively small if the difference between the drying temperature and  $T_g$  is relatively small. As the values of  $\Phi_{ET}(0)$  in Table 3 indicate, if the dispersions dry over a few hours and the drying temperature is room temperature (23 °C), little or no polymer diffusion occurs between the time of film formation and the first fluorescence decay measurement on the sample. On the other hand, latex films with a low extent of cross-linking undergo significant polymer diffusion when dried very slowly at a temperature 30 °C above  $T_g$ . Unannealed films of latex with 0.5% cross-linker exhibit high elongation-to-break and significant toughness. The mechanical properties of this and other latex films improve upon annealing at 80 °C.

Annealing also promotes polymer diffusion. In films formed from cross-linked latex, the extent of polymer mixing through diffusion is limited by the presence of cross-links in each cell. The extent of cross-linking determines both the mean molecular weight between cross-links and the average length of the dangling chains in the system. In Figure 8 we plot the limiting values of  $f_m$  vs calculated values of the number of monomer units between cross-links ( $N_c$ ). In this calculation, we assume that all the double bonds of EGDMA are incorporated as cross-links into the polymer chain. We observe that as  $N_c$  decreases, the limiting value of  $f_m$  also decreases. The effect is striking. The data in Figure 8 suggest an exponential relationship between  $f_m(\text{max})$  and  $N_c$ . The lengths of the looped chains and dangling ends are shorter in films with higher cross-link density. Even small changes in the number of monomers between

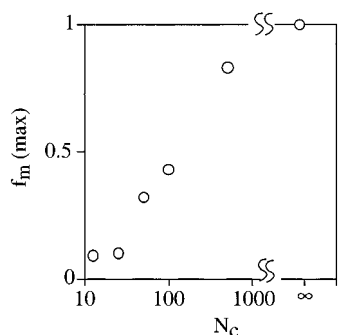


**Figure 8.** Plots of the limiting values of  $f_m$  (fraction of mixing) vs  $N_c$  (number of monomer units between cross-links).

cross-links have a large effect on the extent of polymer diffusion across the boundary between adjacent cells.

Deeper insights into the rate of polymer diffusion are possible through careful examination of the data in Figures 4 and 5. In these two figures we see that  $f_m$  increases in two stages. Initially,  $f_m$  values increase quickly, within 0.5 h for all latex films, reaching values of 0.1–0.3. Subsequently, in films formed from latex containing 0.1–1 mol % EGDMA,  $f_m$  continues to increase, but more slowly, and reaches its maximum value (0.3–0.83) over more than 20 h. This second slower increase in  $f_m$  is not observed in latex films containing 2 and 4 mol % EGDMA. We believe that the first stage involves the interdiffusion of dangling polymer chains at the interparticle boundary and possibly low molecular weight un-cross-linked polymer in the system. The second stage is likely to involve the interdiffusion of long dangling chains that must first disentangle from polymers inside its cell. We picture these processes in Figure 9, where we suggest that long dangling ends, and possibly long loops, near the cell boundary can contribute to diffusion leading to the formation of entanglements.

We end this section with a comparison between the rate of polymer diffusion as monitored by ET measurements and the rate of evolution of the film surface as monitored by AFM. One key example is that of films formed from the latex containing 2 mol % EGDMA. In the unannealed film, we observe a significant surface roughness, with a peak-to-valley distance of about 12–18 nm. The surface becomes nearly flat after 0.5 h annealing, with a peak-to-valley distance of under 0.5 nm. Over the same time period,  $f_m$  reaches its maximum value of 0.1. The film surfaces of newly formed films containing 0.1–0.5 mol % EGDMA have a smaller roughness (3–5 nm) than those of films containing 2 mol % cross-linker. In these films, all indications of surface roughness disappear after 0.5 h annealing at 80 °C. These results are in striking contrast to the growth of ET, a measure of polymer diffusion inside the film, which continues over more than 20 h.

From another perspective, we find that the presence of cross-links has a much larger effect on polymer interdiffusion than on particle deformation. Small extents of latex particle cross-linking (0.1–2 mol %) have only a small effect on particle deformation at the latex surface during film formation. The peak-to-valley distances are much smaller than the particle radii, and deformation is complete within a short annealing time at 80 °C (70 °C above  $T_g$ ). Only at 4 mol % EGDMA is the particle deformation seriously affected. In contrast, more than 0.5 mol % EGDMA significantly limits the extent of polymer interdiffusion inside the film. Defor-

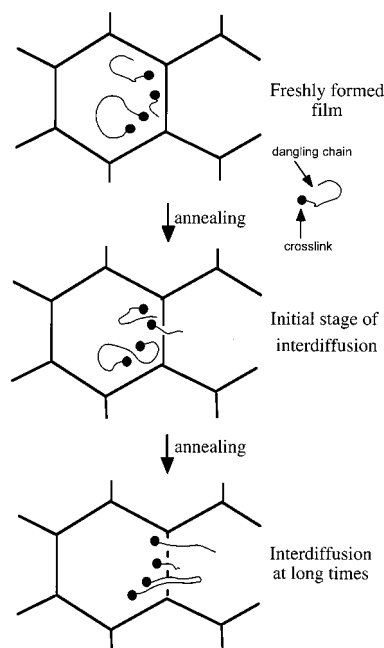


**Figure 9.** Schematic representation of the diffusion process for films formed from cross-linked latex particles. Polymer interdiffusion across a cell boundary proceeds in two stages: For small extents of cross-linking, there is a rapid component to the diffusion, followed by a slower process which we attribute to the time necessary for long loops and dangling chains to first disengage from entanglements within their own cell. For high cross-link densities, this process is no longer important because the dangling ends are too short.

mation at the surface is less sensitive to the extent of cross-linking because elastic deformation can occur without polymer diffusion. This result emphasizes a point first raised by Brown nearly half a century ago.<sup>18</sup>

## Conclusions

In the sections presented above, we show that polymer diffusion can occur across the intercellular boundary between cells of internally cross-linked polymer. The limitations to diffusion imposed by the presence of cross-links emphasize that both mixing and entanglement formation occur as a consequence of diffusion by polymer chains that are connected to the network. The higher the cross-link density, the shorter the length of the dangling chains.

One surprise in our experiments is that, after prolonged annealing, films formed from latex with 4% cross-linking exhibit substantial toughness. This result is very different than that reported by Zosel and Ley for PBMA latex films with about 2% cross-links. A major difference between their experiments, which led to brittle fracture in all films formed from the cross-linked latex, and those reported here is the glass transition temperature of the polymer. Their films had a  $T_g$  slightly above room temperature (ca. 30 °C) whereas our films have a  $T_g$  below room temperature (ca. 10 °C).

None of the films prepared from EGDMA copolymer latex dispersions had any significant solvent resistance. Upon exposure to dioxane at room temperature, the films disintegrated into fragments. The higher the cross-link density, the more fragile the films on exposure to solvent. From this result we infer that solvent swelling promotes disentanglement across the intercellular boundary of loops and ends of the network. Thus, pre-cross-linked latex can improve the tensile properties of a latex

film, but this approach provides no improvement in the solvent resistance. On the basis of our results, however, we can suggest a strategy that may work well to achieve both aims. If the lightly cross-linked latex also contains reactive functionality that permits further cross-linking to take place after film formation and intercellular polymer diffusion, the entanglements formed in this way can be locked in place. Such films should have improved solvent and abrasion resistance in addition to enhanced hardness and tensile strength.

**Acknowledgment.** The authors thank NSERC Canada for their support of this research. We are indebted to Prof. M. Cynthia Goh, Mr. Richard McLoney, and Mr. Bernard Sattin for the AFM measurements, to Dr. Jose-Paulo Farinha and Ms. Ewa Odrobina for helpful discussions about fluorescence decay measurements, and to Mr. Hung Pham for advice about emulsion polymerization.

## References and Notes

- (1) Winnik, M. A. The Formation and Properties of Latex Films. In *Emulsion Polymerization and Emulsion Polymers*; Lovell, P. A., El-Aasser, M. S., Eds.; Wiley: New York, 1997.
- (2) Joanicot, M.; Wong, K.; Cabane, B. *Macromolecules* **1996**, *29*, 4976.
- (3) (a) Buffkin, B. G.; Grawe, J. R. *J. Coat. Technol.* **1978**, *50* (641), 41. (b) Pichot, C. *Makromol. Chem., Macromol. Symp.* **1990**, *35/36*, 327. (c) Park, Y. J.; Kim, J. H. *Polym. Eng. Sci.* **1998**, *38* (6), 884.
- (4) Richard, J.; Wong, K. *J. Polym. Sci., Polym. Phys.* **1995**, *33*, 1395.
- (5) Zosel, A.; Ley, G. *Macromolecules* **1993**, *26*, 2222.
- (6) Hahn, K.; Ley, G.; Oberthur, R. *Colloid Polym. Sci.* **1986**, *264*, 1092; **1988**, *266*, 631.
- (7) Perez, E.; Lang, J. *Langmuir* **1996**, *12*, 3180.
- (8) Ahagon, A. A.; Gent, A. *J. Polym. Sci., Polym. Phys. Ed.* **1995**, *13*, 1285.
- (9) (a) Wang, Y.; Juhué, D.; Winnik, M. A.; Leung, O.; Goh, M. C. *Langmuir* **1992**, *8*, 761. (b) Goudy, A.; Gee, M. L.; Biggs, S.; Underwood, S. *Langmuir* **1995**, *11*, 4454. (c) Butt, H.; Gerharz, B. *Langmuir* **1995**, *11*, 4735. (d) Lin, F.; Meier, D. *J. Langmuir* **1996**, *12*, 2774.
- (10) Goh, M. C.; Juhué, D.; Leung, O.; Wang, Y.; Winnik, M. A. *Langmuir* **1993**, *9*, 1319.
- (11) Zhao, C.; Wang, Y.; Hruska, Z.; Winnik, M. A. *Macromolecules* **1990**, *23*, 4082.
- (12) Feng, J. Ph.D. Thesis, University of Toronto, 1998.
- (13) Kim, H. B.; Winnik, M. A. *Macromolecules* **1994**, *27*, 1779.
- (14) Kim, H. B.; Winnik, M. A. *Macromolecules* **1995**, *28*, 2033.
- (15) Pinenq, P.; Juhué, D.; Winnik, M. A. *J. Coatings Technol.*, submitted for publication.
- (16) Wang, Y.; Zhao, C.-L.; Winnik, M. A. *J. Phys. Chem.* **1991**, *95*, 2143.
- (17) Fox, T. G. *Bull. Am. Phys. Soc.* **1956**, *1*, 123.
- (18) Ahmad, N. M.; Heatley, F.; Lovell, P. A. *Macromolecules* **1998**, *31*, 2822.
- (19) Brown, G. L. *J. Polym. Sci.* **1956**, *22*, 423.
- (20) Mazur, S. In *Polymer Powder Processing*; Rosenzweig, N. M., Ed.; Wiley: New York, 1995.
- (21) Feng, J.; Pham, H.; Stoeva, V.; Winnik, M. A. *J. Polym. Sci., Polym. Phys.* **1998**, *36*, 1129.
- (22) Feng, J.; Winnik, M. A.; Siemiarczuk, A. *J. Polym. Sci., Polym. Phys.* **1998**, *36*, 1115.
- (23) For Area( $\infty$ ), we used the value obtained from solvent-cast films which were prepared from a 1:1 mixture of donor- and acceptor-labeled (1 mol %) non-cross-linked latex dispersions, assuming the state of ideal complete mixing of cross-linked latex is equal to that of the corresponding non-cross-linked latex.
- (24) (a) Farinha, J. P. S.; Martinho, J. M. G.; Yekta, A.; Winnik, M. A. *Macromolecules* **1995**, *28*, 6084. (b) Farinha, J. P. S.; Martinho, J. M. G.; Kawaguchi, S. K.; Yekta, A.; Winnik, M. A. *J. Phys. Chem.* **1996**, *100*, 12552.
- (25) Feng, J.; Odrobina, E.; Winnik, M. A. *Macromolecules* **1998**, *31*, 5290.
- (26) For example, see: Keddie, J. L.; Meredith, P.; Jones, R. A. L.; Donald, A. M. *Macromolecules* **1995**, *28*, 2673.
- (27) (a) Wool, R. P.; O'Conner, K. M. *J. Appl. Phys.*, **1981**, *52*, 5194. (b) Kim, Y. H.; Wool, R. P. *Macromolecules* **1983**, *16*, 1115.

MA990369C